

Spatial superposition at a millimetre scale length using a levitated ferromagnetic nanoparticle

A. T. M. Anishur Rahman*
Department of Physics and Astronomy
University College London
Gower Street, WC1E 6BT London, UK
(Dated: June 19, 2022)

The superposition principle is one of the main tenets of quantum mechanics. In the past, it has been experimentally verified using electrons, photons, atoms, and molecules. However, a similar experimental demonstration using a nano or micro particle is still missing and many proposals have been put forward in the literature for creating such a state. In the existing proposals, the attainable spatial separations between the delocalized states are less than the size of the particles that have been used to create such states. In this article, using a 50 nm levitated ferromagnetic particle and existing technologies, we show that a spatial separation of 1 mm between the superposed states is readily achievable. This may lead to the possibility of testing quantum gravity, collapse models and gravity induced state reduction.

Introduction: Quantum and classical mechanics are the two very successful theories of nature. The dynamics of the microscopic world can be described using the quantum mechanical laws while that of macroscopic world can be predicted using the classical or Newtonian mechanics; meaning all dynamical events in our everyday life can be described using Newtonian mechanics and one can know the precise motion and position of an object at the same time with the full certainty. On the contrary, quantum mechanics predicts [1] that, irrespective of their size or mass, an object can be in multiple states at once and this is certainly true for microscopic systems [1–4]. Specifically, in the past the quantum superposition principle has been demonstrated using neutrons [5], electrons [1], ions [2] and molecules [3, 4]. In 1996 Monroe et al. created a Schrodinger cat state in which they put a beryllium ion in two different spatial locations separated by 80 nm at the same time [2]. They achieved this by levitating a beryllium ion in an ion trap and cooling its center of mass (CM) motion to the ground state. They showed that the internal states were entangled with motional degrees of freedom. The size of the beryllium ion or the Schrodinger cat state was approximately 0.1 nm in size ($\approx 1.5 \times 10^{-26}$ kg). In another experiment [4], tetraphenylporphyrin molecules with high kinetic energy were sent through different grating structures and the resulting matter-wave interfered after a free flight due to the wave nature of matter. In this case, the wave packet of tetraphenylporphyrin was delocalized by hundred times of its diameter. The current record for the largest spatial superposition is 0.5 m which was realized using a Bose-Einstein condensate of Rubidium atoms in an atomic fountain [6], while the heaviest object so far put into a superposition state is about 1×10^{-23} kg [4].

Increasing the macroscopicity of a spatial superposition state is an ongoing global effort and many proposals have been put forward using clamped [7] and levitated optomechanical systems [1, 7–12]. In the levitated

schemes [9, 11, 12], nano-objects are levitated using laser light and spatial superpositions are created and detected using different exotic schemes. Here it is noteworthy that the spatial separations between the two arms of the superposed states that can be achieved are less than the size of the respective objects (≈ 100 nm). Nevertheless, a successful experimental demonstration of such a state using a mesoscopic system can resolve the apparent conflict between quantum mechanics and general relativity [1]. A demonstration of the quantum superposition principle using a mesoscopic object can also shed light on the gravity's role on the quantum state reduction [13]. An additional ramification of an experimental demonstration of a mesoscopic superposition state includes the tests of different collapse models [14].

In this article, we theoretically show that the spatial separation of a quantum superposed state can be increased significantly by using existing technologies. To achieve this, we exploit recent progress, the optical spin polarization of ferrimagnetic or ferromagnetic materials [15–17], that has been made in the magnetic recording industry. In particular, we use all optical helicity dependent switching for flipping spin states of ferrimagnetic or ferromagnetic materials. Exploiting this helicity dependent spin polarization, a pragmatic magnetic field gradient, and a levitated nanosphere, we show that, in principle, a separation of at least 1 mm between the delocalized superposed states is within our reach.

Spatial superposition: A schematic of the proposed experiment is shown in Fig. 1. In the proposed scheme a single domain ferromagnetic or ferrimagnetic particle is levitated using an ion trap. Spins in a single domain ferrimagnetic or ferromagnetic nanoparticle are strongly interacting, highly correlated and perfectly ordered in the ground state due to the strong exchange coupling among the electrons [18, 19]. Consequently, the spins of a single domain ferrimagnet or ferromagnet can be considered as a single superspin and can be described using magnetiza-

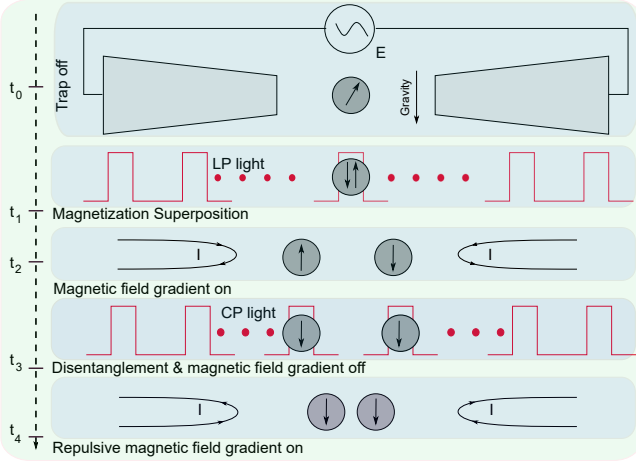


FIG. 1. Experimental setup and the sequence of events- (i) ion trap off, (ii) creation of magnetization superposition using linearly polarized (LP) light, (iii) magnetic field gradient on, (iv) magnetic field off, (v) disentanglement using circularly polarized (CP) light and (vi) matter wave interference that detects spatial superposition.

tion M_s [18–22]. After levitation, the CM temperature of the nanoparticle is parametrically [23] cooled to ≈ 1 K. Subsequent to this, the ion trap is turned off and using all-optical helicity dependent switching, a superposition of magnetization is created. Specifically, it has been experimentally demonstrated that a right $|R\rangle$ (left $|L\rangle$) circularly polarized femtosecond laser pulse produces an up $|\uparrow_{M_s}\rangle$ (down $|\downarrow_{M_s}\rangle$) spin state in certain ferrimagnetic or ferromagnetic i.e. GdFeCo, CoPt, FePtAgC, TbCo, and FePt films containing many domains. In contrast, in the same film, a linearly polarized $(|R\rangle + |L\rangle)/\sqrt{2}$ light pulse creates up and down spin-polarized domains [15–17] - *which is a spin superposition state after wave function collapse*. Although the exact mechanism responsible for this phenomenon is not clearly understood yet [24–26], an enhanced spin-orbit coupling resulted from the exposure to the circularly polarized femtosecond laser pulse is believed to be responsible for this effect [25, 27]. Accordingly, the overall Hamiltonian including the exchange coupling is given by [25]

$$H = \sum_i \left[\frac{\mathbf{p}_i^2}{2m_e} + \frac{1}{2} m_e \Omega_e^2 \mathbf{r}_i^2 + \lambda \mathbf{L}_i \cdot \mathbf{S}_i - e \mathbf{E}(t) \cdot \mathbf{r}_i - \sum_j J_{ij} \mathbf{S}_i \cdot \mathbf{S}_j \right], \quad (1)$$

where m_e , e , Ω_e are the electronic mass, charge, and oscillation frequency, respectively. Furthermore, \mathbf{r}_i , \mathbf{p}_i , \mathbf{L}_i and \mathbf{S}_i are the position, the momentum, the angular momentum, and the spin operators, respectively. Finally, J is the exchange coupling strength with $J > 0$ for ferromagnet and $J < 0$ for ferrimagnet. Figure 2 shows

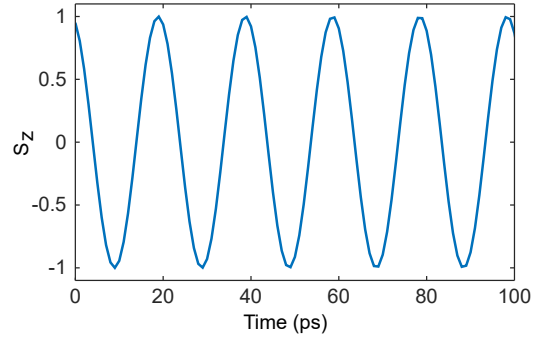


FIG. 2. Magnetization switching from an up state to a down state due to spin-orbit torque [25]. Here, instead of a pulse laser, a CW laser has been used for the purpose of simplicity.

the evolution of a spin system containing ten spins upon exposure to left circularly polarized light under Hamiltonian (1). It can be seen that the spin switches from an initial up state to a down state in about 10 ps.

To create a magnetization superposition $(|\uparrow_{M_s}\rangle + |\downarrow_{M_s}\rangle)/\sqrt{2}$, once the trap is switched off, a femtosecond linearly polarized (LP) laser pulse is applied. Subsequent to this, an inhomogeneous magnetic field is turned on and the particle evolves under the influence of gravitational and magnetic fields for a suitable time $t = t_3 - t_2$. At this state the Hamiltonian is [12]

$$\hat{H} = \frac{\hat{p}_0^2}{2m} + V M_s \frac{dB}{dx} \hat{S} + mg\hat{z}, \quad (2)$$

where m , V and M_s are the mass, volume and magnetization of the levitated particle, respectively. dB/dx is the magnetic field gradient and g is the gravitational acceleration. The spatial separation between the two arms of a superposed states after time t is [12]

$$\Delta x = \frac{M_s t^2}{\rho} \frac{dB}{dx}. \quad (3)$$

It is evident that Δx is independent of mass and hence the spatial separation given by it is valid for an arbitrarily large object and is limited by the coherence time τ and the magnetization of the relevant material.

Detection: After the desired separation Δx between the superposed states $|\phi\rangle = (|\uparrow_{M_s}\rangle|\phi_L(-x_l)\rangle + |\downarrow_{M_s}\rangle|\phi_R(x_r)\rangle)/\sqrt{2}$ is achieved, a disentangling circularly polarized light pulse is activated and the initial magnetic field gradient is switched off. A right (left) circularly polarized light pulse reduces a superposed state into an up (down) spin state [11]. The state of the system at this stage is $|\phi_S\rangle = (|\phi_L(-x_l)\rangle + |\phi_R(x_r)\rangle)/\sqrt{2}$. At this stage, to reduce the free evolution time, another magnetic field is switched on which redirects the separated wave packets towards the center. The duration of this field is adjusted

such that when it is switched off, the spatial separation between the two wave packets is $2x_0 < \Delta x = x_r + x_l$. At the center, the two wave packets interfere to produce an interference pattern. Specifically, let the two arms of the superposed states evolve in free space for an additional time $t_f = t_5 - t_4$. After this free flight, the two arms of the spatially separated non-classical states interfere [3, 11] on a substrate just like in Young's double slit experiment. This interference pattern is used as the signature of spatial superposition created earlier. The period of the interference pattern is given by [11] - $2\pi\hbar t_f / (mx_0)$. The evidence of superposition can also be detected using Ramsey interferometry [12].

Results and discussion: Magnetic order in ferrimagnetic or ferromagnetic materials is a quantum effect and is primarily determined by the exchange interaction [28]. In a crystal lattice, the exchange interaction can be represented as $-\sum_{i \neq j} J \mathbf{S}_i \cdot \mathbf{S}_j$, where J is the strength of the exchange coupling and \mathbf{S}_i and \mathbf{S}_j are the spin operators of the neighbouring i th and j th atoms. For ferromagnetic material $J > 0$ and is approximately 1 eV [27, 29]. In another word, to flip a spin in a ferromagnetic system it requires about $50k_B T_c$, where T_c is the Curie temperature (for FePt $T_c \approx 750$ K [28]). Due to this high energy cost, even at room temperature, permanent magnets can maintain their magnetic order [28, 29]. When atoms with spins are arranged in a crystalline lattice, other interesting phenomena such as domains and magnetocrystalline anisotropy (easy and hard axes) arise [29]. While the magnetocrystalline anisotropy arises from the interaction between the crystalline field and the spin-orbit coupling [29] and determines the preferential orientation of the spins, the origin of the domain formation dwells into the minimization of the energy of the system. That is a ferrimagnetic or ferromagnetic system minimizes the magnetostatic energy by orienting the neighbouring regions into domains of opposite spin. However, when the physical dimension of a magnetic system is reduced below a critical length scale, determined by the balance between the magnetostatic and anisotropy energies, a magnetic system can be monodomain and all the spins in such a system point in a single direction [29]. Although the average size of a monodomain depends on the particle size and shape, it can be on the order of a micrometer [29]. In a cobalt film, a monodomain of size $0.04 \times 1.5 \times 10 \mu\text{m}^3$ has been demonstrated [30] while in CoPt the size of a single domain is about $r = 500$ nm [31].

Coherence: Coherence time is characterized by using two time constants i.e. spin-lattice relaxation time T_1 and transverse relaxation time T_2 , and in general $T_2 \leq 2T_1$ [32]. While T_1 is determined by the spin-lattice interaction, T_2 is primarily fixed by the inhomogeneities and fluctuation in magnetic and crystal fields. For homogeneous isotropic material $T_1 = T_2$ [32, 33]. In ferromagnetic materials, the usage of T_1 and T_2 is not prevalent rather Gilbert damping α , which characterizes how

a spin system loses energy and angular momentum, is widely used [34–36]. Nevertheless, α , T_1 and T_2 are intricately related with each other [36, 37]. In the absence of any inhomogeneities [37], valid for small nanocrystals, coherence time is given by $\tau = 1/(\alpha\gamma B)$, where B is the magnetic field and γ is the gyromagnetic ratio. In a recent experiment Capua et al. [36] have measured both α and τ using a polycrystalline bulk CoFeB film sandwiched between multiple capping layers at room temperature. The coherence time of the overall film, $20 \times 20 \mu\text{m}^2$ in size, was about 0.5 ns but it was increased to ≈ 15 ns when a subset of the spins was selected. α in this film was 0.029. Rabi oscillation, a *purely quantum phenomenon and a precursor for the current proposal*, in this film, has also been demonstrated for the first time [36]. In a polycrystalline bulk FePt film at room temperature, α as low as $\approx 1 \times 10^{-2}$ has been recorded [38] while ferrimagnetic yttrium iron garnet (YIG) has the lowest [39] $\alpha = 9 \times 10^{-5}$. A direct substitution of $\alpha = 9 \times 10^{-5}$, $B = 1$ T in $\tau = 1/(\alpha\gamma B)$ provides a coherence time in excess of 11 μs . Since a single domain ferrimagnetic or ferromagnetic nanocrystal 10 – 100 nm in size, such as FePt, GdFeCo and CoFe is considered in this article, longer coherence times are expected. Levitation, a physical contactless low noise environment, may boost the coherence time further. Additionally, performing the experiment at a cryogenic temperature will increase the coherence time significantly. A cryogenic temperature is also beneficial for suppressing magnons [28] which is another mechanism that shortens the coherence time. It is also important to mention that due to the finite size of the magnetic nanoparticles considered in this letter, magnons will be heavily damped and only the high energy oscillations can be excited [19].

Example: Although all optical helicity dependent switching has been demonstrated using many different materials, in this article we use ferromagnetic face centred tetragonal (L1₀) FePt. It has one of the highest magnetocrystalline anisotropy [40] and is readily available in monodisperse single domain nanocrystalline form [40–42]. Single domain FePt particles $r \approx 100$ nm has been synthesized in the past as well [43]. All optical helicity dependent switching has also been recently demonstrated in laboratories [44] using this material. Ferromagnetism, a manifestation of quantum exchange coupling, of FePt guarantees that all the spins contained within a levitated particle are exchange-coupled and hence behave as a single coherent macrospin rather than a multitude of product states. Furthermore, a high magnetocrystalline anisotropy of FePt [40] ensures a vanishingly small thermal flipping of spins. A strong magnetization (M_s) of FePt is also essential for achieving a large separation between the superposed states. FePt is also preferable due to most of the naturally abundant isotopes of iron ($\approx 98\%$) and platinum ($\approx 70\%$) are nuclear spin free which guarantees enhanced spin coherence time [32, 33].

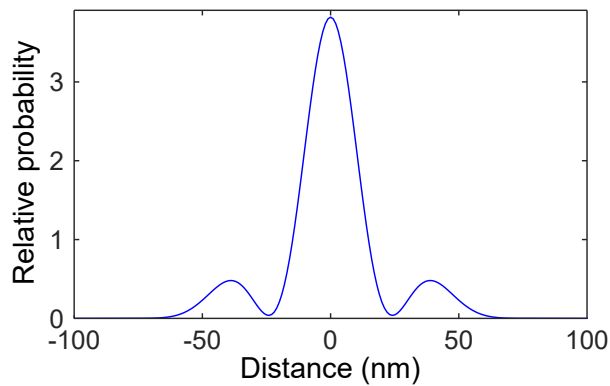


FIG. 3. Matter wave interference after a free-flight of $t_f = 100$ ms. Parameters used are $r = 25$ nm, $\beta \approx 3$ nm and the separation between the two arms is approximately $2x_0 = 10$ nm.

To provide a numerical example of achievable separation between the superposed states, let us consider a FePt particle of radius $r = 25$ nm which is levitated and prepared as described before. Assuming $M_s = 1.8 \times 10^5 \text{ JT}^{-1} \text{ m}^{-3}$ [42], $\frac{dB}{dx} = 1 \times 10^5 \text{ Tm}^{-1}$, $\rho = 4000 \text{ kg m}^{-3}$ and $t = 10 \text{ } \mu\text{s}$, one gets $\Delta x \approx 1$ mm. This is a macroscopic distance and can be identified using the naked eye. The magnetic field gradient used in this calculation is realistic and indeed much more conservative than readily available using the current technologies [45]. Figure 3 shows the relevant matter-wave interference pattern generated after the free evolution of the two arms of the spatial superposition states for 100 ms. This interference pattern can be visualized using an electron microscope.

It is noteworthy that the coherence time that has been used for the previous calculation may seem higher than the measured values in the literature. However, most of the measured coherence times were deduced from macroscopic thin films containing many domains and grains [36, 38, 39] and consequently does not reflect the true coherence time of a single domain monocrystalline ferrimagnet or ferromagnet. Furthermore, these measurements were performed at room temperature while in this article we are interested at temperatures around that of liquid helium (≈ 4 K). As a result, a longer coherence time is viable and the time used in the calculation is justified.

Macroscopicity: In the scale of macroscopicity [10], the combination of the particle mass and spin coherence time used in the previous example amounts to $\mu = 18.5$. Nevertheless, this can be significantly increased by using a single domain [31] CoPt particles ($r = 500$ nm) and for which all optical helicity dependent switching has also been demonstrated [17]. In this case, macroscopicity is ≈ 26 . Here, we note that the matter-wave interference

pattern used for the confirmation of the spatial superposition is not suitable for larger particles. This is due to the fact that the separation between the fringes in the matter-wave interference pattern diminishes significantly as the particle size/mass increases making matter-wave interference unsuitable. However, to circumvent this, one can use Ramsey interferometry based detection scheme which is independent of the particle mass or size [12].

Conclusions: In this article we have theoretically demonstrated that using a levitated single domain ferrimagnetic or ferromagnetic nanoparticle and all optical helicity dependent switching, a spatial superposition state can be created. In this scheme, the spatial separation between the two arms of a superposition state is ≈ 1 mm. This is about four orders of magnitude larger than those available in other proposals in the literature. Superposition states of ferrimagnetic or ferromagnetic nanoparticles proposed in this article can be used for quantum computing and quantum-enhanced sensing.

* a.rahman@ucl.ac.uk

- [1] M. Arndt and K. Hornberger, Nat. Phys. **10**, 271 (2014).
- [2] C. Monroe, D. M. Meekhof, B. E. King, and D. J. Wineland, Science **272**, 1131 (1996).
- [3] M. Arndt, O. Nairz, J. Vos-Andreae, C. Keller, G. V. D. Zou, and A. Zeilinger, Nature **401** (1999).
- [4] S. Eibenberger, S. Gerlich, M. Arndt, M. Mayor, and J. Txen, Phys. Chem. Chem. Phys. **15**, 14696 (2013).
- [5] M. Zawisky, M. Baron, R. Loidl, and H. Rauch, Nucl. Instrum. Methods Phys. Res. **481**, 406 (2002).
- [6] T. Kovachy, P. Asenbaum, C. Overstreet, C. A. Donnelly, S. M. Dickerson, A. Sugarbaker, J. M. Hogan, and M. A. Kasevich, Nature **528**, 530 (2015).
- [7] J. D. Teufel, T. Donner, D. Li, J. W. Harlow, M. S. Allman, K. Cicak, A. J. Sirois, J. D. Whittaker, K. W. Lehnert, and R. W. Simmonds, Nature **475** (2011).
- [8] W. Marshall, C. Simon, R. Penrose, and D. Bouwmeester, Phys. Rev. Lett. **91**, 130401 (2003).
- [9] O. Romero-Isart, A. C. Pflanzer, F. Blaser, R. Kaltenbaek, N. Kiesel, M. Aspelmeyer, and J. I. Cirac, Phys. Rev. Lett. **107**, 020405 (2011).
- [10] S. Nimmrichter and K. Hornberger, Phys. Rev. Lett. **110**, 160403 (2013).
- [11] Z. Yin, T. Li, X. Zhang, and L. Duan, Phys. Rev. A **88**, 033614 (2013).
- [12] C. Wan, M. Scala, G. W. Morley, A. T. M. A. Rahman, H. Ulbricht, J. Bateman, P. F. Barker, S. Bose, and M. S. Kim, Phys. Rev. Lett. **117**, 143003 (2016).
- [13] R. Penrose, Gen. Rel. Gravit. **28**, 581 (1996).
- [14] A. Bassi, K. Lochan, S. Satin, T. P. Singh, and H. Ulbricht, Rev. Mod. Phys. **85**, 471 (2013).
- [15] C. D. Stanciu, F. Hansteen, A. V. Kimel, A. Kirilyuk, A. Tsukamoto, A. Itoh, and T. Rasing, Phys. Rev. Lett. **99**, 047601 (2007).
- [16] S. Mangin, M. Gottwald, C.-H. Lambert, D. Steil, V. Uhl, L. Pang, M. Hehn, S. Alebrand, M. Cinchetti, G. Malinowski, Y. Fainman, M. Aeschlimann, and E. E. Fullerton, Nat. Mater. **13** (2014).

- [17] C.-H. Lambert, S. Mangin, B. S. D. C. S. Varaprasad, Y. K. Takahashi, M. Hehn, M. Cinchetti, G. Malinowski, K. Hono, Y. Fainman, M. Aeschlimann, and E. E. Fullerton, *Science* **345**, 1337 (2014).
- [18] D. D. Awschalom, D. P. DiVincenzo, and J. F. Smyth, *Science* **258**, 414 (1992).
- [19] Y. Tabuchi, S. Ishino, T. Ishikawa, R. Yamazaki, K. Usami, and Y. Nakamura, *Phys. Rev. Lett.* **113**, 083603 (2014).
- [20] E. M. Chudnovsky and L. Gunther, *Phys. Rev. Lett.* **60**, 661 (1988).
- [21] D. D. Awschalom, J. F. Smyth, G. Grinstein, D. P. DiVincenzo, and D. Loss, *Phys. Rev. Lett.* **68**, 3092 (1992).
- [22] C. C. Rusconi, V. Pöschhacker, K. Kustura, J. I. Cirac, and O. Romero-Isart, *Phys. Rev. Lett.* **119**, 167202 (2017).
- [23] P. Nagornykh, J. E. Coppock, and B. E. Kane, *Appl. Phys. Lett.* **106**, 244102 (2015).
- [24] M. S. E. Hadri, M. Hehn, G. Malinowski, and S. Mangin, *J. Phys. D* **50**, 133002 (2017).
- [25] G. P. Zhang, T. Latta, Z. Babyak, Y. H. Bai, and T. F. George, *Mod. Phys. Lett. B* **30** (2016).
- [26] A. Kirilyuk, A. V. Kimel, and T. Rasing, *Rev. Mod. Phys.* **82**, 2731 (2010).
- [27] G. P. Zhang, Y. H. Bai, and T. F. George, *EPL* **115**, 57003 (2016).
- [28] J. M. D. Coey, *Magnetism and magnetic materials* (Cambridge University Press, Cambridge ; New York, 2009).
- [29] C. L. Dennis, R. P. Borges, L. D. Buda, U. Ebels, J. F. Gregg, M. Hehn, E. Jouguelet, K. Ounadjela, I. Petej, I. L. Prejbeanu, and M. J. Thornton, *J. Phys. Condens. Matter* **14**, R1175 (2002).
- [30] E. Seynaeve, G. Rens, A. V. Volodin, K. Temst, C. Van Haesendonck, and Y. Bruynseraede, *J. Appl. Phys.* **89**, 531 (2001).
- [31] O. Gutfleisch, J. Lyubina, K. H. Müller, and L. Schultz, *Adv. Eng. Mater.* **7**, 208 (2005).
- [32] I. Žutić, J. Fabian, and S. Das Sarma, *Rev. Mod. Phys.* **76**, 323 (2004).
- [33] F. Bloch, *Phys. Rev.* **70**, 460 (1946).
- [34] J. M. Beaujour, D. Ravelosona, I. Tudosa, E. E. Fullerton, and A. D. Kent, *Phys. Rev. B* **80**, 180415 (2009).
- [35] M. Schoen, D. Thonig, M. Schneider, T. Silva, H. Nembach, O. Eriksson, O. Karis, and J. Shaw, *Nat. Phys.* **12**, 839 (2016).
- [36] A. Capua, C. Rettner, S.-H. Yang, T. Phung, and S. S. Parkin, *Nat. Commun.* **8** (2017).
- [37] A. Capua, S.-h. Yang, T. Phung, and S. S. P. Parkin, *Phys. Rev. B* **92**, 224402 (2015).
- [38] S. Iihama, S. Mizukami, N. Inami, T. Hiratsuka, G. Kim, H. Naganuma, M. Oogane, T. Miyazaki, and Y. Ando, *Jpn. J. Appl. Phys* **52**, 073002 (2013).
- [39] H. Chang, P. Li, W. Zhang, T. Liu, A. Hoffmann, L. Deng, and M. Wu, *IEEE Magn. Lett.* **5**, 1 (2014).
- [40] S. Sun, C. B. Murray, D. Weller, L. Folks, and A. Moser, *Science* **287**, 1989 (2000).
- [41] X. Teng and H. Yang, *J. Am. Chem. Soc.* **125**, 14559 (2003).
- [42] H. L. Nguyen, L. E. M. Howard, G. W. Stinton, S. R. Giblin, B. K. Tanner, I. Terry, A. K. Hughes, I. M. Ross, A. Serres, and J. S. O. Evans, *Chem. Mater.* **18**, 6414 (2006).
- [43] G. Q. Li, H. Takahoshi, H. Ito, H. Saito, S. Ishio, T. Shima, and K. Takanashi, *J. Appl. Phys.* **94**, 5672 (2003).
- [44] R. John, M. Berritta, D. Hinzke, C. Müller, T. Santos, H. Ulrichs, P. Nieves, J. Walowski, R. Mondal, O. Chubykalo-Fesenko, J. McCord, P. Oppeneer, U. Nowak, and M. Münzenberg, *Sci. Rep.* **7**, 4114 (2017).
- [45] C. Tsang, C. Bonhote, Q. Dai, H. Do, B. Knigge, Y. Ikeda, Q. Le, B. Lengsfeld, J. Lille, J. Li, S. MacDonald, A. Moser, V. Nayak, R. Payne, N. Robertson, M. Schabes, N. Smith, K. Takano, P. van der Heijden, W. Weresin, M. Williams, and M. Xiao, *IEEE Trans. Magn.* **42**, 145 (2006).